GEOPHYSICAL RESEARCH LETTERS, VOL. 25, NO. 5, PAGES 729-732, MARCH 1, 1998

Current collection at the shuttle orbiter during TSS-1R high voltage charging

V.M. Agüero,[1] S.D. Williams,[1] B.E. Gilchrist,[2] L. Habash Krause,[2]
D.C. Thompson,[3] W.J. Raitt,[3] W.J. Burke,[4] and L.C. Gentile[5]

Abstract. We compare measurements of collected currents and Space Shuttle Orbiter potentials, taken during the Tethered Satellite System (TSS) missions, with predictions of a numerical model. The model assumes thin potential sheaths about the Orbiter and contributions from both ram and thermal currents. It was originally developed to explain the smaller than expected Orbiter charging detected throughout the first TSS mission (TSS–1). During periods of the TSS reflight (TSS–1R) when the Orbiter potential was > -100 V the model effectively described current collection. Deviations from model predictions appeared at more negative potentials. These indicate bounds of applicability for the model and the growing importance of unaccounted physical processes. Data acquired near the time of the tether break suggest that additional current during the break was carried by secondary ions created in collisions between surface-generated electrons and ambient neutrals within the Orbiter's high-voltage sheath.

Introduction

Spacecraft charging, critical for understanding plasma measurements in both the ionosphere and magnetosphere, remains a topic of much active research [*Anderson et al.*, 1994; *Garrett and Whittlesey*, 1996; *Machuzak et al.*, 1996]. NASA plans to use large, electrically active spacecraft in low earth orbit as platforms for scientific and engineering experiments created a need to understand how complex vehicles such as the Space Shuttle Orbiter and the international space station charge and collect current. The Tethered Satellite System missions (TSS–1 in 1992 and TSS–1R in 1996) provided opportunities to study the steady-state levels of charging required by the Orbiter to extract large currents from ionospheric plasmas. The accurate control and measurement capabilities of TSS instrumentation facilitated empirical studies of the charging of this large, complex spacecraft [*Dobrowolny and Stone*, 1994; *Agüero et al.*, 1994; *Agüero*, 1996].

The TSS instrumentation and mission goals are described comprehensively by *Stone and Bonifazi* [1997] and *Dobrowolny and Stone* [1994]. TSS–1 and TSS–1R were cooperative missions conducted by NASA and the Italian Space Agency in which an electrically conducting satellite of 1.6 m diameter was deployed upward from the payload bay of the Orbiter. The two vehicles were connected by an electrically conducting tether which was insulated from the plasma. The orbital motion of this system across the Earth's geomagnetic field induced an EMF, $\phi_{\rm EMF}$, that could be used to drive a current through the tether. The electron current from the ionosphere to the satellite must be balanced by an equal flux of positive ions collected at the Orbiter or by the emission of electrons (*e.g.* by electron guns located on the Orbiter). During the deployed phase of each TSS mission the Orbiter was oriented with its largest conducting surfaces, the main engine nozzles, facing the ram direction.

For the purposes of this study it is useful to consider the TSS as operating in two distinct modes. In its "low impedance" mode, electrons collected at the satellite flowed through the tether. If the ion flux reaching conducting surfaces of the Orbiter was less than the tether current, the Orbiter charged negatively. In the second mode, the tether and the Orbiter were either electrically disconnected or they were connected through a high impedance resistor (*cf.* Figure 1 of *Gentile et al.* [1997]). Two techniques could be used to determine the Orbiter's potential $\phi_{\rm orb}$ with respect to the local plasma. Direct measurements were made from spectral peaks observed in ion fluxes detected by the Shuttle Potential and Return Electron Experiment (SPREE) located in the payload bay [*Machuzak et al.*, 1996; *Gentile et al.*, 1997]. Potentials could also be inferred by applying Ohm's law for the TSS circuit:

$$-\phi_{\rm orb} - \phi_{\rm EMF} + i_{\rm tether}(R_{\rm T} + R_{\rm O}) + \phi_{\rm sat} = 0 \qquad (1)$$

where $i_{\rm tether}$ is the measured current flowing through the tether, $R_{\rm T}$ is the resistance of the tether, $R_{\rm O}$ represents the resistance imposed between the tether and the Orbiter, and $\phi_{\rm sat}$ is the satellite potential relative to

[1]Space, Telecomm., and Radiosci. Lab, Stanford Univ.
[2]Space Physics Research Lab, University of Michigan
[3]Center for Atm. and Space Sci., Utah State University
[4]Phillips Laboratory, Hanscom Air Force Base
[5]Boston College Institute for Scientific Research

Paper number 97GL02948.
0094-8534/98/97GL-02948$05.00

its local plasma environment. In the "high impedance" mode the potential measured between the Orbiter and the tether was very close to the full motional EMF. Investigations by *Agüero* [1996] and *Williams et al.* [1997] demonstrate our ability to model accurately the induced EMF voltage and thereby identify other superposed contributions to the measured voltage.

This study focuses on the deployed phases of the TSS–1 and TSS–1R missions when the tether and the Orbiter were electrically coupled by a resistor, R_O, of either 15 Ω or 25 kΩ, depending on tether length. Data were used from intervals when no electron gun was operating. In these cases the Orbiter charged negatively with respect to its local plasma. Orbiter charging and ambient plasma density data acquired during these intervals were used as inputs to a numerical model of Orbiter current collection developed to assist the analysis of TSS–1 measurements [*Agüero*, 1996]. We show that at the higher charging magnitudes achieved during TSS–1R, the current collected by the Orbiter greatly exceeded model predictions based on the low-voltage TSS–1 results. The most extreme example occurred during a 9 s interval prior to the tether break when the tether short circuited to the Orbiter's frame [*Gilchrist et al.*, 1997]. Simultaneous SPREE particle measurements in the payload bay suggest that the additional current was carried by secondary ions created in collisions between surface-generated electrons and ambient neutrals within the high-voltage sheath.

Analysis and Results

Values of ϕ_{orb} were measured by the SPREE and computed using Ohm's law. In calculating ϕ_{orb} we used R_T values of 2.0 kΩ for TSS–1 and 1.8 kΩ for TSS–1R [*Thompson et al.*, 1997]. Plasma densities and satellite potentials were recorded by a satellite Langmuir probe and a DC Boom Package, respectively [*Dobrowolny et al.*, 1994]. We direct attention to two points: (1) Measured and inferred values of ϕ_{orb} are quite consistent [*Agüero*, 1996; *Gentile et al.*, 1997], although there are fewer SPREE measurements for TSS–1 because of the lower charging magnitudes recorded on that mission. With its minimum energy channel at 9.8 eV, the SPREE could not measure Orbiter potentials within the ±10 V range [*Gentile et al.*, 1997]. (2) The data show that the generally higher magnitudes of ϕ_{orb} encountered during TSS–1R resulted both from the greater tether length and consequent ϕ_{EMF} and also the large tether currents that the satellite was able to extract from its plasma environment [*Stone and Bonifazi*, 1997].

Prior to the TSS missions it was believed the tether currents would be approximately equal to the Orbiter's ram current collection [*Banks*, 1989]. Because of the Orbiter's limited ability to collect ion currents, i_{tether} would be small and most of ϕ_{EMF} would appear as high values of ϕ_{orb}. Data from TSS–1 disproved this conjecture and led to the development of a new current-collection model for the Orbiter which we will refer to as A-96 [*Agüero*, 1996]. This model was developed from first principles for thin-sheath, current collection, but with a significant empirical difference from the preflight models. The principal improvement in A-96 is the inclusion of the conducting surface of the satellite deployer boom, an ~12 m long thin lattice, that had not previously been considered. Detailed measurements of all Orbiter conducting surfaces and their sheath geometries were incorporated into this model. Thus, A-96 accounts for ram, sheath, and thermal currents to conductors and avoids multiple counting in the overlapping sheath regions between boom lattice members and between the Orbiter's main engine nozzles.

The equation defining the sheath thickness t_{sh} is

$$t_{sh} = \frac{2}{3}\sqrt{\left(\frac{2}{qm_i}\right)^{\frac{1}{2}}\left(\frac{\epsilon_0 V^{\frac{3}{2}}}{j_B}\right)} \qquad (2)$$

where $V = |\phi_{orb}|$ and $j_B = 1.53\Gamma_{sh}$, is the Bohm-corrected thermal flux across the sheath edge [*Bohm*, 1949]. The conducting surfaces included in A-96 are the Orbiter engine nozzles, payload bay vent-grills, payload bay conducting blankets, and payload conducting surfaces. In the TSS–1 Orbiter attitude these yield ~16 m^2 of conducting surface exposed to the ram currents and ~62 m^2 of conducting surfaces exposed to thermal currents. The basic model assumptions are that: (1) all ram ions entering sheaths are collected, (2) at low charging magnitudes secondary emissions are not significant, and (3) photoemission current density, ~ 10^{-5} A/m^2, contributes negligibly to the daytime current balance compared to measured tether currents [*Agüero*, 1996; *Machuzak et al.*, 1996]. To compare TSS–1R data with A-96 predictions, a simple cosine projection of the conducting area to the ram direction was adopted to account for Orbiter pitch variations of up to 40°. The Orbiter pitch-induced shadowing of payload-bay conductors from the ram plasma flow was also accounted for by a cosine projection into the payload bay of the aft payload bay bulkhead.

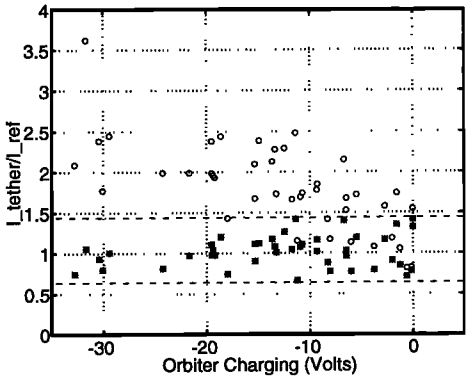

Figure 1. Ratios of TSS–1 tether current normalized by A-96 predictions (*) and Orbiter ram current (o). Measurement uncertainty is bounded by the dashed lines.

Figure 1 shows two representations of tether currents measured during TSS–1 plotted as a function of ϕ_{orb}. The upper set of points, represented by open circles, shows measured tether currents normalized by ram currents to the Orbiter [*Agüero*, 1996]. These points show that current collection at higher charging magnitudes was up to 3.5 times larger than the simply computed ram current levels. The lower set of points shows the measured tether currents normalized by the A-96 predictions for currents to the Orbiter. While deviations from a ratio of 1 remain between the A-96 predictions and the measured tether currents, these were found to be uncorrelated with other variables or mission operations. The dashed lines in Figure 1 represent the maximum range that results from an estimated 20% uncertainty in measured plasma densities (as communicated by the RETE team which derived plasma densities from langmuir probe measurements [*Lebreton*, 1996]).

Figure 2 shows tether currents measured during TSS–1R plotted as a function of ϕ_{orb}. The data are normalized by the A-96 predictions for currents to the Orbiter using the numerically computed sheath and conducting surface areas described previously. Again, the dominant uncertainty derives from errors in measured plasma densities, as indicated by the dashed lines. The points show a trend suggested by the solid curve, derived using a second order polynomial fit to the data points. A good match is obtained between the model and data at low charging levels. The discrepancy between them increases with increasing $|\phi_{orb}|$. The data point labeled "A" was taken in the 9 s prior to the tether break when the i_{tether} approached 1 A and $\phi_{orb} \approx -600$ V [*Gilchrist et al.*, 1997; *Gentile et al.*, 1997]. This demonstrates that the Orbiter was able to collect >9 times more current than predicted by A-96. The point labeled "B" was acquired during Orbiter thruster firings and shows more significant deviations from A-96 than most of the other points. We note that the location of point "B" on the graph is consistent with the inhibition of ion access to the Orbiter by aft thruster firings, requiring a larger value of $|\phi_{orb}|$ to extract less ion current from the ionosphere [*Machuzak et al.*, 1996].

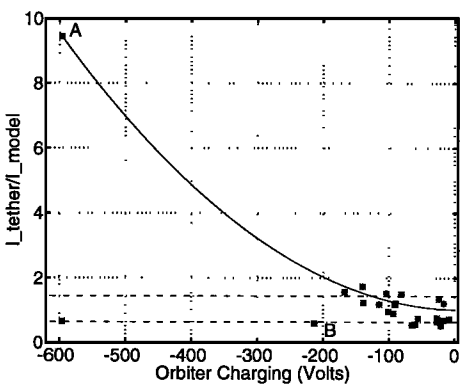

Figure 2. Ratios of TSS–1R tether current normalized by A-96 predictions. Solid curve shows trend of current collection at higher charging levels. Measurement uncertainty is bounded by the dashed lines.

Discussion

In this study we have investigated the Orbiter's ability to collect ion current from the ionosphere as manifested during the TSS missions. We have also tested our ability to predict the relationship between Orbiter charging and ion current collection. The TSS–1R charging analysis showed good agreement with A-96 at low charging levels. Since these conditions are similar to those for which the TSS–1 model was derived this result is gratifying but not surprising. It demonstrates that sheath-augmented ion collection to both large conductors and thin frame conductors cannot be ignored and is adequate for explaining the current collection observations at low charging levels [*Agüero*, 1996]. However, significant deviations from model predictions at higher charging levels suggest that there are bounds of applicability for the numerical model A-96. The current-collection trend in Figure 2, indicated by the solid curve, shows that at large values of $|\phi_{orb}|$, the Orbiter collected more current than estimated by A-96. This trend away from the ram, sheath, and thermal levels of current collection suggests a transition in the physical processes affecting Orbiter current collection. In the regime from approximately -100V to -200V the agreement remains surprisingly good, even though the charging levels are between 3 and 6 times those under which the A-96 model was derived. In the regime represented by the point "A", near the time of the tether break at approximately 17 times the highest charging level shown for the TSS-1 mission, a new process was dominant.

An explanation for the enhancement in plasma current collection to the Orbiter at large negative charging levels is not yet clear. It can be stated that typical current generating mechanisms such as photoemission or secondary emission by themselves are insufficient enhancements. Photoemission currents are too small, and secondary emission, even with an assumed 100% yield, would only double the collected currents, not multiply them by a factor of nine. However, a scenario involving electron emission from a conducting surface does suggest itself.

During the tether-break event, the SPREE measured strong ion spectral peaks with energies near 600 eV. On this basis it was determined that $\phi_{orb} \approx -600$ V, a value corroborated by tether based computed values. At the same time, the SPREE also detected intense fluxes of both ions and electrons with energies below the spectral peak. Figure 3 shows the ion spectrum as measured by the SPREE for this charging event. From considerations of energy conservation, it is clear that few of these ions and none of the electrons originated outside the Orbiter sheath. Electrons emitted from Orbiter surfaces are quickly accelerated away. However, if

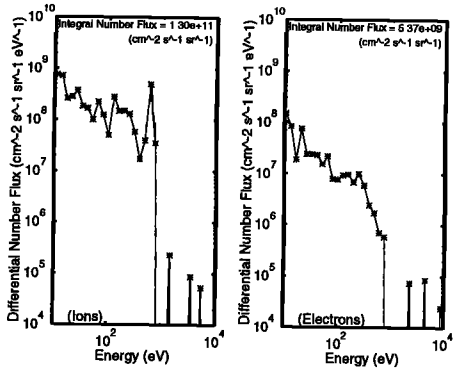

Figure 3. SPREE Head A Fast Sweep ion and electron spectra for the ≈ 600 V Orbiter charging event prior to the tether break. (Time: 057/01:29:17; ESA Azimuth = 156; Peak Zone = 9)

the potential across the sheath approaches 100 V, these electrons become very efficient sources for secondary ionization of neutral atoms or molecules. The neutrals come from the local atmosphere and Orbiter outgassing, with a typical neutral density two orders of magnitude higher than the plasma density and outgassing producing even higher local densities. Figure 8 of *Strickland et al.* [1976] shows that the cross-section for ionization of neutrals by electrons has a broad peak near 100 eV. Ions created in the sheath by the accelerated electrons are attracted to the Orbiter surface, thus contributing to the total collected current. There are then three sources of current to the Orbiter, accelerated ambient ions, emitted electrons and secondary ions. To explain the factor of nine increase in current observed during event "A" the efficiency of secondary ionization must be very high, approaching conditions similar to those of beam-plasma discharge observed in laboratory plasmas [*Papadopoulos*, 1986 (and the references therein)].

Acknowledgments.

This work was supported in part by NASA contracts NAS8-36812 and NAS8-39381. We are grateful for the data from the Research on Electrodynamic Tether Effects (RETE) plasma sensor package provided by the Space Sciences Department (SSD) of ESA/ESTEC. The RETE DC Boom Package (DCBP) satellite charging and Langmuir Probe (LP) plasma density data were contributed by J.-P. Lebreton from the ESA/ESTEC/SSD. Recognition is given to P.M. Banks, D.S. Lauben, P.R. Williamson, and A.B. White for their contributions to the TSS missions.

References

Agüero, V.M., P.M. Banks, B.E. Gilchrist, I. Linscott, W.J. Raitt, D.C. Thompson, V.V. Tolat, A.B. White, S.D. Williams, and P.R. Williamson, The shuttle electrodynamic tether system (SETS) on TSS-1, *Il Nuovo Cimento, 17C(1),* 49, 1994.

Agüero, V.M., A study of electrical charging on large LEO spacecraft using a tethered satellite as a remote plasma reference, PhD thesis, Stanford Univ., June 1996.

Anderson, P.C., W.B. Hanson, W.R. Coley, and W.R. Hoegy, Spacecraft potential effects on the Dynamics Explorer 2 satellite, *J. Geophys. Res., 99(A3),* 3985, 1994.

Banks, P.M., Review of electrodynamic tethers for space science, *J. of Spacecr. Rockets, 26,* 234, 1989.

Bohm, D., *The characteristics of electrical discharges in magnetic fields*, McGraw-Hill, New York, 1949.

Dobrowolny, M. and N.H. Stone, A technical overview of TSS-1: the first tethered satellite system mission, *Il Nuovo Cimento, 17C(1),* 1, 1994.

Dobrowolny, M., *et al.*, The RETE experiment for the TSS-1 mission, *Il Nuovo Cimento, 17C(1),* 101, 1994.

Garrett, H.B. and A.C. Whittlesey, Spacecraft charging: An update (AIAA 96-0143), paper presented at 34th Aerospace Sci. Conf., AIAA Press, Jan. 1996.

Gentile, L.C., W.J. Burke, C.Y. Huang, J.S. Machuzak, D.A. Hardy, D.G. Olson, B.E. Gilchrist, J.-P. Lebreton, and C. Bonifazi, Negative Shuttle Charging during TSS-1R, submitted to *Geophys. Res. Lett.*, TSS-1R Special Section: Part 1, 1997.

Gilchrist, B.E., C. Bonifazi, S.G. Bilen, W.J. Raitt, W.J. Burke, N.H. Stone, and J.-P. Lebreton, Enhanced electrodynamic tether currents due to electron emission from a neutral gas discharge: results from the TSS-1R mission, submitted to *Geophys. Res. Lett.*, TSS-1R Special Section: Part 1, 1997.

Lebreton, J.-P., Analysis method of the Langmuir Probe I-V Characteristics (Rev. 1), *ESA/ESTEC/SSD Internal Note,* 1 Mar. 1996.

Machuzak, J.S., W.J. Burke, L.C. Gentile, V.A. Davis, D.A. Hardy, and C.Y. Huang, Thruster effects on the shuttle potential during TSS-1, *J. Geophys. Res., 101,* 13437, 1996.

Papadopoulos, K., Scaling of beam plasma discharge for low magnetic fields, *J. Geophys. Res., 91,* 1627, 1986.

Stone, N.H. and C. Bonifazi, The TSS-1R mission: overview and scientific context, submitted to *Geophys. Res. Lett.*, TSS-1R Special Section: Part 1, 1997.

Strickland, D.J., D.L. Book, T.P. Coffey, and J.A. Fedder, Transport equation techniques for the deposition of auroral electrons, *J. Geophys. Res., 81,* 2755, 1976.

Thompson, D.C., *et al.*, The current-voltage characteristics of a large probe in low earth orbit: TSS-1R results, submitted to *Geophys. Res. Lett.*, TSS-1R Special Section: Part 1, 1997.

Williams, S.D., B.E. Gilchrist, V.M. Agüero, R.S. Indiresan, D.C. Thompson, and W.J. Raitt, TSS-1R vertical electric fields: Long baseline measurements using an electrodynamic tether as a double probe, submitted to *Geophys. Res. Lett.*, TSS-1R Special Section: Part 1, 1997.

V.M. Agüero and S.D. Williams, STAR Lab/MS-9515, Stanford University, Stanford, CA 94305. (email: aguero@nova.stanford.edu; scott@nova.stanford.edu)

W.J. Burke, Geophysics Directorate, Phillips Laboratory, 29 Randolph Road, Hanscom Air Force Base, MA 01731. (email: burke@plh.af.mil)

L.C. Gentile, Boston College Inst. for Scientific Res., St. Clement's Hall 402, 140 Commonwealth Avenue, Chestnut Hill, MA 02167. (email: gentile@plh.af.mil)

B.E. Gilchrist and L. Habash Krause, Space Physics Res. Lab., 2455 Hayward Ave, Ann Arbor, MI 48109. (email: gilchrst@eecs.umich.edu; quantum@eecs.umich.edu)

D.C. Thompson and W.J. Raitt, CASS/SER218D, Utah State University., Logan, UT 84322. (email: thompson@demise.cass.usu.edu; raitt@cass.usu.edu)

(Received January 16, 1997; revised September 24, 1997; accepted October 13, 1997.)